Article Type: Full Paper

Synthesis, Biological Evaluation and Molecular Docking Studies of Novel 4-Arylpyridin-1(4*H*)-yl) benzoic acid Derivatives as Anti-HIV-1 Agents

Saghi Sepehri,[a,b] Sepehr Soleymani,[c] Rezvan Zabihollahi,[c] Mohammad R. Aghasadeghi,[c] Mehdi Sadat,[c] Lotfollah Saghaie,[a] Afshin Fassihi [a,*]

[a]Department of Medicinal Chemistry, School of Pharmacy and Pharmaceutical Sciences, Isfahan University of Medical Sciences, 81746-73461, Isfahan, Iran
E-mail: fassihi@pharm.mui.ac.ir (A. Fassihi)

[b]Department of Medicinal Chemistry, School of Pharmacy, Ardabil University of Medical Sciences, Ardabil, 5618953141, Iran

[c]Department of Hepatitis and AIDS, Pasteur Institute of Iran, Tehran, Iran

The structural similarities between N1 substituted 1,4-dihydropyridines and the known gp41 inhibitors, **NB-2** and **NB-64**, were considered in the current research for the design of some novel anti-HIV-1 agents. A series of novel 4-arylpyridin-1(4H)-yl) benzoic acid derivatives were synthesized and after a comprehensive structural elucidation were screened for *in vitro* anti-HIV-1 activity. Most of the tested compounds displayed moderate to good inhibitory activity against HIV-1 growth and were evaluated for *in vitro* cytotoxic activity using XTT assay at the concentration of 100 μM. Among the tested compounds, **1c**, **1d** and **1e** showed potent anti-HIV-1 activity against P24 expression at 100 μM with inhibition percentage of 84.00, 76.42 and 80.50 %, respectively. All the studied compounds possessed no significant cytotoxicity on MT-2 cell line. The binding modes of these compounds to gp41 binding site were determined through molecular docking study. Docking studies proved **1a** as the most potent compound and binding maps exhibited that the activities might be attributed to the electrostatic and hydrophobic interactions and additional H-bonds with the gp41 binding site. The Lipinski's ''rule of five'' and drug-likeness criteria were also calculated for the studied compounds. All derivatives obeyed the Lipinski's ''rule of five'' and had drug-like features. The findings of this study suggest that novel 4-arylpyridin-1(4*H*)-yl) benzoic acid might be a promising scaffold for the discovery and development of novel anti-HIV-1 agents.

Keywords: Anti-HIV-1• N1 substituted 1,4-dihydropyridines• Gp41• Docking simulation

Introduction

Despite many developments in the prevention and treatment, HIV-1 still remains a universal health challenge due to the continued evolution of resistance to medications presently provided to combat it. The first anti-retroviral drug was presented in the mid-1980s. It was a nucleotide mimic inhibiting HIV-1 reverse transcriptase enzyme. Today, 25 anti-HIV drugs acting on different viral targets have been approved for the treatment of AIDS. A drug protocol called highly-active antiretroviral therapy (HAART) applies a combination of anti-retroviral drugs, generally including two different nucleoside reverse transcriptase inhibitors (NRTIs) and an non-nucleoside reverse

transcriptase inhibitor (NNRTI) or a protease inhibitor.[1] Because of the serious adverse effects, drug resistance and increased number of patients of HIV-1 infection who fail to respond to HAART, development of novel anti-HIV-1 drugs is necessitated.[2],[3]

Viral entry, the first step of HIV-1 infection, is a promising step for anti HIV-1 drug design.[4],[5] It consists of the attachment of the viral and target cell membranes, a procedure mediated by a series of molecular events involving viral envelope proteins, gp120 and gp41.[6] The trans-membrane subunit of glycoproteins 41 (gp41) includes extracellular and trans-membrane domains and an intra-cytoplasmic tail. The trans-membrane domain contains a hydrophobic N-terminal fusion peptide followed by a polar region, an N-terminal heptad repeat (NHR), a disulfide-bridged loop region, a C-terminal heptad repeat (CHR), and a membrane-proximal external region.[7],[8] During fusion, binding of gp120 to CD4 and chemokine receptors (CXCR4 or CCR5) on the target cell results in conformational changes that disrupt the interactions between gp41 and gp120, upon this the buried trans-membrane protein gp41 will be exposed. After exposure of gp41, the NHR region (trimer) zips around a preformed trimer of CHR helix and packs in an anti-parallel manner to form a six-helix bundle (6-HB).[7],[9],[10]

The first entry inhibitor approved for clinical use, enfuvirtide (also referred to as T20), is a peptide that inhibits fusion.[8] Clinical application of the enfuvirtide and other peptides are limited due to their high production cost, poor pharmacokinetic profile and induction of drug resistance.[9] Two non-peptide pyrrole derivatives, **NB-2** and **NB-64** (**Fig.1**), were presented by high-throughput screening technique as new HIV-1 fusion inhibitors in 2004. These compounds bind to the gp41 protein via ionic and hydrophobic interactions.[10],[11] There is a hydrophobic pocket inside the gp41 binding site and the interaction of the six helix bundle (6-HB) with the residues of this pocket is critical for the stability of the helix. This pocket is considered as a hotspot for small molecule drug design. It can accommodate compounds with a molecular mass of 500 to 600 Da. Small-molecule compounds that target this pocket have been identified in several reports.[12]

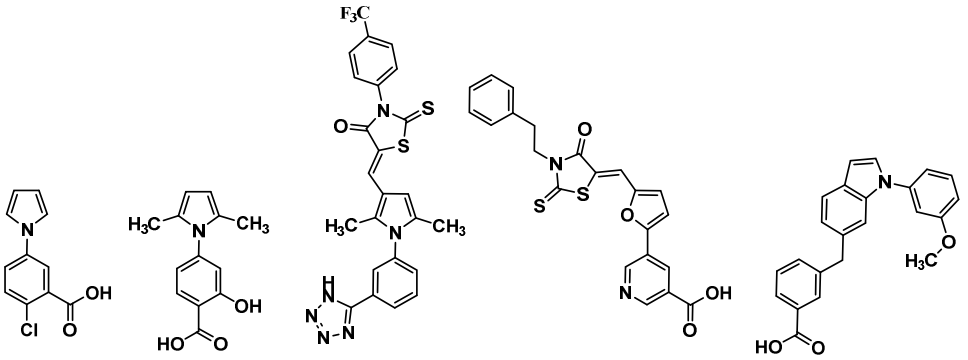

Figure 1. Some small-molecule HIV-1 fusion inhibitors

Molecular docking analysis of **NB-2** and **NB-64** indicates that each of them occupy only a part of the deep hydrophobic pocket on the gp41 NHR trimer.[13] These compounds are small and do not fill the pocket. Compounds with increased hydrophobicity and additional H-bonding functionalities provide the necessary affinity required for a small molecule inhibitor (compounds **1**, **2** and **3**; **Fig.1**).[14],[15] These compounds provide an expanding linear binding conformation thus occupy more space in the binding pocket.[13],[14]

Some structural similarities can be observed between **NB-2** and **NB-64** as recognized gp41 inhibitors and 1,4-dihydropyridine derivatives for anti-HIV-1 activity. Most of the gp41 inhibitors such as **NB-2** and **NB-64** have a -COOH moiety in their scaffold able to form salt bridges with positively charged residues (Lys574 or Arg579) located in the gp41 binding site. Aromatic rings in the structures of gp41 inhibitors as hydrophobic moieties have shown good interactions with the hydrophobic pocket of the gp41 binding site enhancing the potency.[13-15] Based on this, the anti-HIV-1 activity of 1,4-dihydropyridines containing a phenyl ring substituted on the N1 and a (het)aryl moiety located on the C4 position of 1,4-DHP scaffold was considered in our research group. Our preliminary molecular docking studies showed that a -COOH functionality on the para position of the phenyl ring significantly influences the orientation of the compound in the gp41 binding site. It has been reported that carboxylic acid moiety in most of the gp41 inhibitors binds electrostatically to the Lys574 or Arg579 residues located on the surface of the groove pocket in gp41 structure. It is verified that removing this group will reduce the anti-HIV-1 potency of the compound. Another key structural feature of **NB-2** and **NB-64** which is involved in the interaction with hydrophobic binding surface of the gp41 is the two intersecting rings, pyrrol and the substituted phenyl rings. This system of **NB** structures has an analogue in 1,4-DHP compounds: the substituted phenyl ring attached to the N1 atom

of the 1,4-DHP scaffold. The substituted aromatic ring attached to the nitrogen atom of 1,4-DHP ring increases the hydrophobicity and molecular size. This scaffold is supposed to occupy the hydrophobic pocket inside the gp41 binding site efficiently which favors the anti-HIV-1 activity according to previous researches.

There are few reports on the anti-HIV-1 activity of 1,4-dihydropyridine derivatives. Hilgeroth and coworkers have reported N-substituted cage dimeric 4-aryl-1,4-dihydropyridines as a novel class of HIV-1 protease inhibitors in 1999. The compounds they investigated exerted 6-32% inhibition at 25 and 50 μM on the activity of HIV-1 protease.[16] In another work, the same researchers prepared a series of novel N-H and N-alkyl-substituted cage dimeric 4-aryl-1,4-dihydropyridines. As HIV-1 protease inhibitors their IC_{50}s were between 16.1 to 262 μM.[17]

1,4-dihydropyridine derivatives have been reported as anti-HIV-1 agents working by moderate inhibition of HIV-1 protease.[18] There is not any report for the inhibition of HIV-1 gp41 by 1,4-dihydropyridine scaffold.

In this paper we report the design, synthesis, and *in vitro* HIV-1 inhibitory activity of some novel N1 substituted 1,4-dihydropyridine compounds: 4-(3,5-bis(alkoxycarbonyl)-2,6-dimethyl-4-arylpyridin-1(4*H*)-yl)benzoic acid derivatives. The structural similarities with known gp41 inhibitors were considered in the design of these compounds. Intermolecular interactions of the studied compounds with the putative viral receptor, gp41, were also investigated using molecular docking simulations.

Results and Discussion

As it was mentioned in the introduction, the most relevant compounds which were previously reported as anti-HIV-1 compounds were dimeric dihydropyridine derivatives. They were evaluated as inhibitors of HIV-1 protease enzyme. They were different from the compounds in the present study in both the chemical structure and the biological target. In the following sections the *in vitro* and *in silico* results of anti-HIV-1 studies of the prepared compounds are discussed in detail.

Chemistry

Symmetric N1 substituted 1,4-dihydropyridine derivatives (**1a-h**) were synthesized as described in **Scheme 1**. The core 1,4-DHP ring was constructed according to the Hantzsch multi-component cyclocondensation reaction.[19] In brief, a mixture of the proper aldehyde, alkyl acetoacetate and *para*-amino benzoic acid was refluxed in absolute ethanol to provide 4-[3,5-bis(alkoxycarbonyl)-2,6-dimethyl-4-arylpyridin-1(4H)-yl] benzoic acid derivatives (**1a-h**). For compounds **1b** and **1h** the reaction was complete when HCl was used as a catalyst.

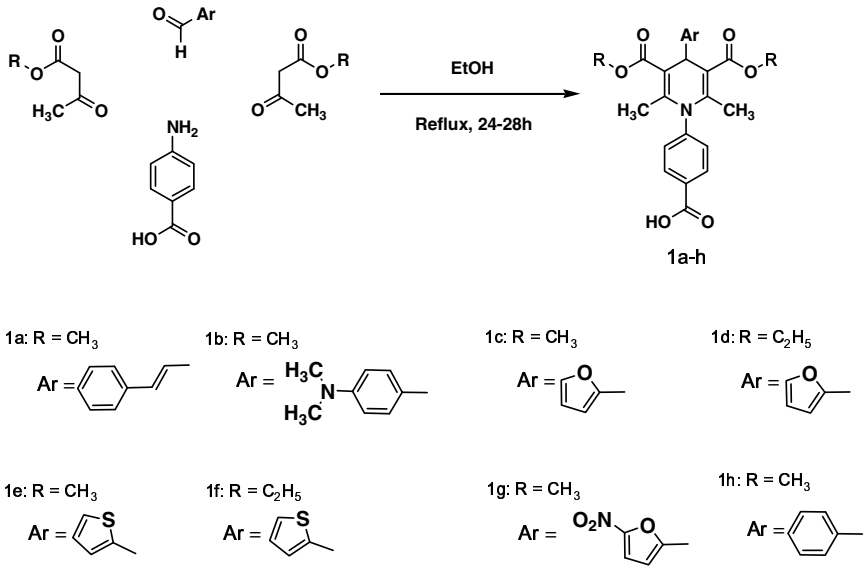

Scheme 1. Synthesis of 4-[3,5-bis(alkoxycarbonyl)-2,6-dimethyl-4-arylpyridin-1(4H)-yl] benzoic acids (**1a-h**).

Structures of compounds **1a-h** were unambiguously established on the basis of their spectral (^{1}H-NMR, FT-IR and LC-Mass) and elemental analysis data. FT-IR spectra of the final compounds exhibited the characteristic broad absorption peaks of carboxylic acid O-H group around 2500-3500 cm^{-1}. Stretch absorption bands of carboxylic acid C-O were also observed in 1072-1315 cm^{-1}. The presence of the ester and carboxylic acid C=O groups was confirmed by strong absorption peaks at 1686-1705 cm^{-1} and 1609-1677 cm^{-1}, respectively. ^{1}H-NMR spectra revealed broad singlets at 10.63-13.27 ppm demonstrating the presence of carboxylic acid group in the final compounds. Singlet peaks in 4.83-5.91 ppm belonging to the C-4 proton of the DHP ring confirmed that this ring is formed successfully. Other ^{1}H-NMR spectral signals were in accordance with the proposed structures.

Biological assay

Anti-HIV activities of all the synthesized derivatives were evaluated in terms of inhibitory activity against HIV-1 replication in HEK cells cultures. All the synthesized compounds were also tested for their cytotoxicity on MT-2 cell line by XTT assay. Evaluated compounds did not exhibit significant cytotoxicity at concentrations below 100 μM. HIV-1 replication inhibitory activities at 100 μM from 27 to 84% were recorded for the studied compounds. The biological results are summarized in Table **1**.

Relationships between the structure and the anti-HIV-1 activity of the synthesized derivatives were as follows:

1) Compounds **1c** and **1d** showed higher activity when compared with other derivatives. It can be postulated that hetero aromatic groups at C4 position might be responsible for the higher activity of these compounds.These compounds possess 2-furyl heterocyclic substituent instead of substituted phenyl ring at C4 of the 1,4-DHP scaffold. One possible reason may be related to additional H-bonding ability of 2-furyl moiety. This is also reflected in the TPSA of these compounds which is 106.29 $Å^2$. The same postulation has been made by other researchers.[14] Ligand-receptor interaction plots showed that oxygen atom of 2-furan hetero-aromatic ring at C4 position of 1,4-DHP is involved in hydrogen bonding with indole NH of Trp571. Replacement of the furyl substituent in compound **1c** with thienyl (compound **1e**) lowered the activity. According to the 2D ligand-receptor interaction plots, sulfur atom is not involved in hydrogen bonding with any of the gp41 binding site residues; instead, it has additional hydrophobic interactions with the target.

Table 1. Anti-HIV-1 activity of the prepared compounds

Compound	100 μM	
	(%) inhibition rate of P_{24} expression	% cell viability
1a	30.57 ± 4.08	86.63 ± 1.52
1b	47.50 ± 2.50	93.37 ± 4.15
1c	84.00 ± 0.17	82.12 ± 2.04
1d	80.50 ± 1.63	98.15 ± 2.20
1e	76.42 ± 5.69	75.16 ± 5.09
1f	50.12 ± 7.50	96.30 ± 2.99
1g	30.00 ± 5.00	80.55 ± 5.57
1h	27.00 ± 7.96	65.72 ± 2.86
BMS-806	100	100

[a] F=22.66303 > F Crit=3.500464, *p*-value=0.000113
[b] F=9.703489 > F Crit=3.500464, *p*-value=0.002322

2) An explanation for the lower activity of compounds **1a**, **1b** and **1h** might be the inappropriate orientation of styryl and phenyl derivatives at C4 position of 1,4-dihydropyridine scaffold in the gp41 binding site. This can be seen in **Fig.2** by superimposing **1a** and **1c** in the gp41 binding site.

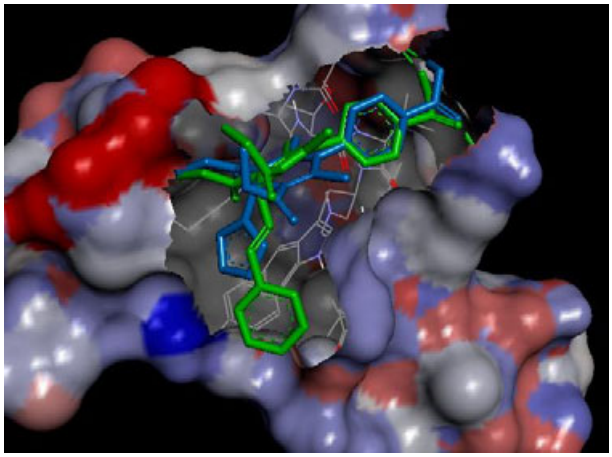

Figure 2. Superimposition of **1a** (green sticks) and **1c** (blue sticks) from docking results.

3) Compound **1g** with 5-nitro-2-furyl heterocyclic ring at C4 of the 1,4-DHP ring showed weak antiviral activity which might be attributed to the decreased lipophilicity of the compound due to the presence of nitro group at C5 position of the 2-furyl ring. Literature reports have shown that the presence of more than one -COOH group in the compound leads to a decreased inhibitory activity.[15] On the basis of such rationalization, the presence of both nitro and carboxylic acid groups in compound **1g** might be inappropriate for inhibitory activity.

4) The lower activity of compound **1f** (bearing ethoxy carbonyl moiety at C3 and C5 positions of the core scaffold) in comparison with compound **1e** (bearing methoxy carbonyl at the same positions) was thought to be due to the difference in the lipophilicity of the compounds.

In silico studies

In silico calculation of physicochemical parameters and toxicity studies

As a part of the present investigation, a computational study was performed for estimating the drug-likeness and bioavailability of compounds. One of the key goals in drug design is to identify potent molecules which possess a rational absorption, distribution, metabolism and excretion (ADME) profile, *i.e.*, drug-like molecules. The Lipinski's rule of five measures of drug-likeness which is critical for rational drug design was applied in determining drug-likeness. This rule states that most molecules with good membrane permeability should have calculative partition coefficient values (CLogP) in the octanol-water system ≤ 5, molecular weight (MW) ≤ 500, number of hydrogen bond acceptors ≤ 10 and number of hydrogen bond donors ≤ 5. Compounds that satisfy this rule are considered as drug-like ones. Thus, compounds with the number of violations not more than 1 display good bioavailability. In addition to these four criteria, some more measures are nowadays considered to determine the drug-likeness of the molecules. Topological polar surface area (TPSA), logarithm of aqueous solubility in terms of mol/L (LogS), number of rotatable bonds, and seven more criteria were also determined in this study as measures of drug-likeness. Numerical values for all of these criteria are given in Tables **2** and **3**. On the basis of in silico drug-likeness study, all compounds obeyed Lipinski's rule of five and compounds **1c** and **1e** did not have any violations from the rule of five.

Table 2. Calculated pharmacokinetic parameters

Compound	TPSA	CLogP	n-ROTB	HBA	Volume	Lipinski's violations
1a	93.1	6.14	8	7	405.6	1
1b	96.4	5.59	8	8	424.1	1
1c	106.3	4.27	7	8	359.8	0
1d	106.3	5.02	9	8	393.4	1
1e	93.1	4.91	7	7	368.9	0
1f	93.1	5.67	9	7	402.5	1
1g	152.1	4.35	8	11	383.1	1
1h	93.1	5.49	7	7	378.2	1

TPSA (•2), topological polar surface area; CLogP, logarithm of compound partition coefficient between n-octanol and water; n-ROTB, number of rotatable bonds; HBA, number of hydrogen bond acceptors. Number of hydrogen bond donors (HBD) for the studied compounds was 1.

Table 3. Prediction of anti-HIV-1 compounds as drug-like molecules

Compound	LogS[a]	Drug-likeness	Drug-score[b]	M[c]	T[d]	IR[e]	RE[f]
1a	-4.74	-1.85	0.32	NO	NO	NO	NO
1b	-4.30	-1.53	0.13	NO	YES	NO	YES
1c	-3.95	-0.76	0.47	NO	NO	NO	NO
1d	-4.55	-2.20	0.33	NO	NO	NO	NO
1e	-4.28	0.80	0.54	NO	NO	NO	NO
1f	-4.88	-0.56	0.35	NO	NO	NO	NO
1g	-4.99	-0.82	0.14	YES	YES	NO	NO
1h	-4.27	-0.27	0.46	NO	NO	NO	NO

[a] More than 80% of the drugs on the market have an estimated logS (logarithm of aqueous solubility measured in M) value greater than -4; [b] drug score combines drug likeness, CLogP, logS, molecular weight and toxicity risks; [c] Mutagenicity; [d] Tumorigenicity; [e] Irritant effect; [f] Reproductive effect.

Molecular flexibility measured by the number of rotatable bonds (optimally below 8) is another important predictor of good oral bioavailability. According to data in Table **2**, all of the synthesized derivatives had an optimum number of rotatable bonds (<8) except **1d** and **1f** (number of rotatable bonds = 9) as they obtain a moderate degree of structural rigidity.

Toxicity risk (mutagenicity, tumorogenicity, irritation, and reproduction) are signals alarming that the calculated compounds may be harmful concerning the risk category specified. Most of the compounds did not show any potential of toxicity in toxicity risk assessment (Table **3**).

In Osiris calculations the drug-likeness prediction is a fragment based approach. A positive drug-likeness value states that a molecule contains mainly fragments which are often present in commercial drugs. Osiris study displayed that compound **1c** had a high positive drug-likeness value, and the fragments of this compound had a contribution for drug-like activity.

The studied compounds revealed moderate to good drug score introducing them as potentially safe lead compounds. Drug-likeness and drug-score values of the designed compounds are presented in Table **3**.

Molecular docking study

Molecular docking as an important methods in structure-based computer-assisted drug design predicts the main binding mode(s) of a ligand with a protein of known three-dimensional structure.[20] From another aspect of view, docking simulation could be applied to find the binding mode and mechanism of more active derivatives. Molecular docking simulation of the interaction with gp41 was carried out to investigate the posible inhibition of this protein with the prepared compounds. 4-(3,5-Bis(alkoxycarbonyl)- 2,6-dimethyl-4-arylpyridin-1(4*H*)-yl)benzoic acids (**1a-h**) were all docked into the gp41. Docking results are summarized in Tables **5** and **6**.

Docking results showed that evaluated structures possessed similar binding modes in gp41. Observed binding modes were associated with different docking scores. Previous SAR studies on other chemical series revealed that three major contact motifs recognizable within the gp41 binding pocket are as follows:

a) Flexible and positively-charged Lys574 and Arg579 residues which could form a strong salt bridge with the negatively charged carboxylic group of the ligands

b) Hydrophilic amino acids which could form hydrogen bonds (e.g. Gln567 and Gln575)

c) Hydrophobic amino acids providing favorable hydrophobic interactions.

These three key contact motifs may lead to the inhibition of gp41 6-helix bundle formation. **NB-2** and **NB-64** have been identified as drug-like compounds during the screening of small-molecule libraries in the recent years.[21] At the first step of docking, we focused on exploring the binding mode of both **NB-2** and **NB-64** within the entire protein via a blind-docking procedure to validate the applied docking protocol. The obtained results showed that the docked compounds were located in a groove containing Trp571, Gln575, Leu581, Gln577, Lys574, Leu568 and Gln567 residues of gp41. An electrostatic interaction between the carboxylate group of each ligand and Lys574 as well as a hydrogen bond between the hydroxyl group of **NB-2** and Gln567 in gp41 was observed.[11] These blind-docking results were in accordance with the previous reports.[10,22] Subsequent to the validation of the docking protocol, the 3D structures of 4-(3,5-bis(alkoxycarbonyl)-2,6-dimethyl-4-arylpyridin-1(4*H*)-yl)benzoic acid derivatives (**1a-h**) were all docked into gp41 protein. The following ligand-receptor interaction features were derived from the obtained docking results:

1) Previous researches suggested that compounds with improved anti-HIV-1 potency could be obtained by increasing the molecular size and hydrophobicity since they can occupy the hydrophobic pocket efficiently.[23],[24] In the present study, the substituted aromatic ring attached to the nitrogen atom of 1,4-DHP ring increases the hydrophobicity and molecular size which favors the anti-HIV-1 activity (Table **3**).

2) Electrostatic interaction with the positively-charged amino acids of gp41 (Lys574 and/or Arg579) which is crucial for the receptor inhibition is provided by *para*-carboxylic acid substitution on the phenyl ring at N1 position of 1,4-DHP. *para*-Carboxylic acid substitution on all 1,4-DHP derivatives contributed to form a strong salt bridge with Lys574 and/or Arg579.

3) In almost all the docked 1,4-dihydropyridine structures, hydrogen bond with Gln567 or Gln575 can be detected.

4) It was observed that most of the studied compounds had almost similar binding orientation in gp41 binding site. However, they had slightly different binding modes. The *in silico* binding mode of the two most active compounds (**1c** and **1d**) against gp41 can be seen in **Fig.3**.

5) Compounds **1a**, **1b** and **1g** showed the highest binding energy. It seemed that the styryl and 4-dimethylamino phenyl substituent on the C-4 position of 1,4-DHP ring of **1a** and **1b** might be responsible for additional hydrophobic interactions with the gp41 binding site. In the case of **1g**, the high binding free energy was for the increased electrostatic interactions due to the presence of the nitro group. As mentioned earlier, the improper permeability as a result of high TPSA made this compound less active in anti-HIV-1 evaluations.

6) Nitro group substituted on furyl ring at C4 position of 1,4-DHP ring (**1g**) could be responsible for additional electrostatic interaction with NH of Lys574 through oxygen atom of a nitro substituent (**Fig.4**).

Table 4. Interactions between the docked 1,4-dihydropyridine derivatives and gp41 binding site residues.

Compound	Hydrogen bond			Amino acids in non-bonded contacts	Amino acids in electrostatic contacts
	Amino acid	Distance (Å)	Angle (°)		
1a	Lys574, Gln567	1.77 1.95	133.81 26.42	Lys574, Gln567, Trp571, Leu568, Val570, Trp631, Glu630,Glu634	Lys574
1b	Lys574, Gln567	1.74 2.15	146.01 34.58	Lys574, Gln567, Trp571, Leu568, Val570, Trp631, Glu630,Glu634	Lys574
1c	Lys574, Gln567, Trp571	1.94 1.90 2.98	37.82 30.59 66.83	Lys574, Gln567, Trp571, Leu568, Val570, Trp631, Glu630,Glu634	Arg579
1d	Lys574, Arg579, Gln575	1.93 3.09, 1.88 2.12	149.49 112.69,134,84 28.08	Arg579, Lys574, Gln575, Ala578, Gln577, Trp571	Arg579
1e*	Lys574, Gln567, Trp571	1.81 2.12 2.39	130.22 5.81 41.35	Lys574, Gln567, Trp571, Leu568, Val570, Trp631	Lys574
1f	Lys574, Arg579, Gln575	2.37 1.84 2.10	141.01 135.92 26.38	Arg579, Lys574, Gln575, Ala578, Gln577, Trp571	Arg579
1g	Lys574, Arg579, Gln575	2.15 3.06 1.84 2.22	121.22 112.98 161.99 11.09	Arg579, Lys574, Gln575, Ala578, Gln577, Trp571	Lys574, Arg579
1h	Lys574, Gln567	1.71 2.13	132.20 43.23	Lys574, Gln567, Trp571, Leu568, Val570, Trp631, Glu634	Lys574
BMS-806	Lys574, Trp571	1.89 2.98	11.42 64.82	Lys574, Gln567, Trp571, Leu568, Glu634, Trp631	-

*__1e__ had cation-π interaction with Lys574 residue inside the active site.

Table 5. Docking results of 1,4-dihydropyridine derivatives docked into fusion HIV-1 virus target (gp41, PDB ID: 1AIK)

Compound	$\Delta G_{binding}$ [a] (kcal/mol)	Intermol energy (kcal/mol)	Electrostatic energy (kcal/mol)	Vdw_Hbond_desolv energy (kal/mol)
1a	-5.82	-8.51	-1.20	-7.31
1b	-5.75	-8.44	-1.12	-7.32
1c	-5.33	-7.46	-1.22	-6.23
1d	-5.29	-8.28	-1.37	-6.91
1e	-4.25	-6.64	-0.97	-5.67
1f	-4.96	-7.94	-1.12	-6.82
1g	-5.76	-8.44	-2.44	-6.01
1h	-5.56	-7.94	-1.21	-6.73
BMS-806	-6.42	-7.61	-0.19	-7.42

[a] F=0.152896 < F Crit=2.069832, p-value= 0.99598

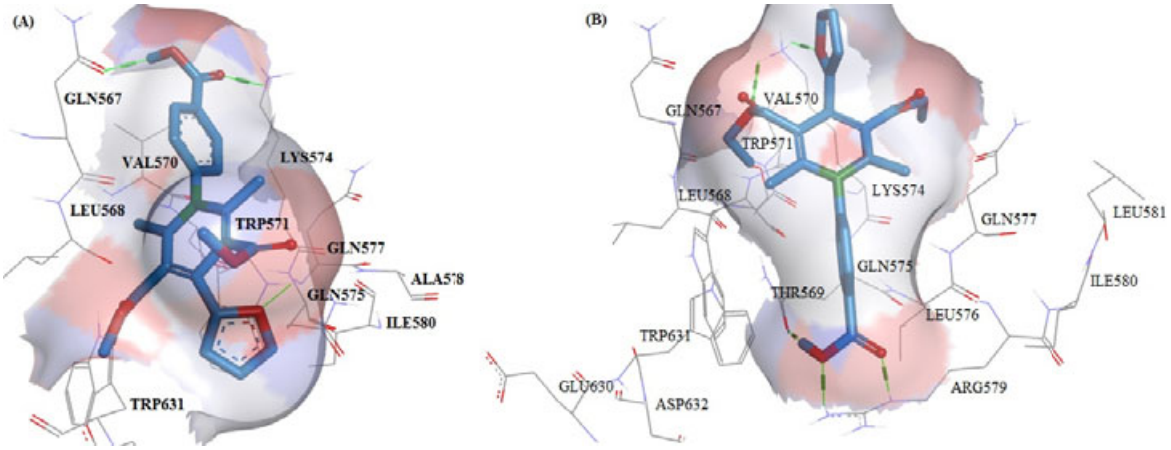

Figure 3. Compounds **1c** (A) and **1d** (B) in gp41 binding site.

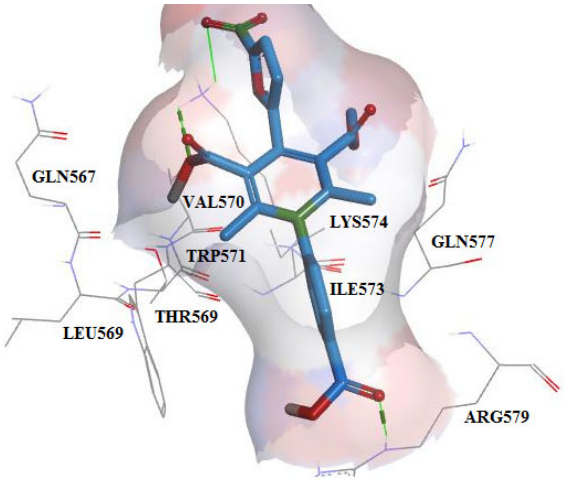

Figure 4. Compound **1g** at binding site of gp41

7) Carboxylic acid groups of **1c**, **1d**, **1e** and **1g** showed electrostatic interaction with Arg579, while in other compounds Lys574 was involved in such an interaction.

8) Oxygen atom of the 2-furyl and sulfur atom of the 2-thiophenyl hetero-aromatic substituents at the C4 position of 1,4-DHP (compounds **1c**, **1d** and **1e**, **1f**) had a determinant role in H-bond interactions with Lys574.

9) Different H-bond patterns were observed for the studied compounds. For **1a**, **1b**, **1c**, **1e** and **1h** hydrogen bond was formed with Gln567, while compounds **1d**, **1f** and **1g** participated in hydrogen bonding to Gln575.

10) Oxygen atom of methyl esters at C3 and C5 of the 1,4-DHP ring in **1e** and furyl ring at C4 position of **1c** participated in H-bond interaction with Trp571.

11) All the 1,4-DHP structures participated in non-bonded interactions with Trp571, Leu568, and Val570 residues. Compounds **1d**, **1f** and **1g** also showed additional hydrophobic contacts with Ala578.

12) Docking results showed that Trp631, Glu630 and Glu634 contributed to non-bonded contacts with **1a**, **1b**, **1c** and **1h** (Table **4**) while they did not show any hydrophobic contacts with **1d**, **1f** and **1g**.

13) Compounds **1d**, **1f** and **1g** formed hydrophobic interactions with Gln577 located inside the binding pocket.

14) Compound **1e** was found to take part in a cation-π stacking interaction with Lys574, while, other compounds did not show such an interaction.

15) Compound **BMS-806** was docked in gp41 binding site and showed interactions almost similar to **NB-2** and synthesized derivatives. This compound forms H-bond with Lys574 and Trp571. It was not able to interact electrostatically with the receptor since it lacks the proper functionalities (**Fig.5**).

As illustrated in **Scheme 2**, compounds **1c-e** showed HIV-1 inhibitory activity up to 70%. The inhibitory activity of the reference compound (**BMS-806**) was 100% at the same concentration. Other compounds displayed moderate activity (**Scheme 2**). This suggests that novel N1-substituted 1,4-DHP derivatives are good candidates for further HIV-1 inhibition studies. In addition, results of **Scheme 3** showed that all of the compounds exhibited docking results comparable to **NB-2**. Finally, it was found that compound **1c** (2-furyl ring at C4 position of 1,4-DHP and methyl ester moieties at C3 and C5 positions of 1,4-DHP) was the most potent compound in HIV-1 inhibition assay. Compound **1a** (styryl group at C4 position of 1,4-DHP) showed the highest $\Delta G_{binding}$ in molecular docking study.

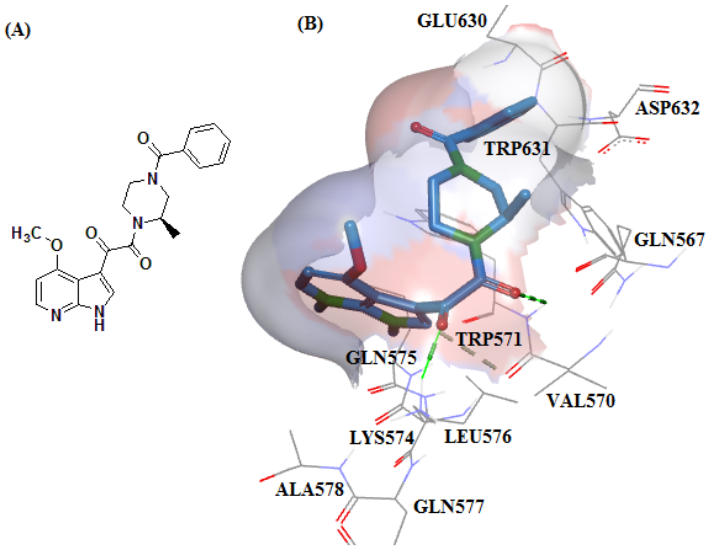

Figure 5. A. Chemical structure of **BMS-806**, **B.** Compound **BMS-806** at gp41 binding site

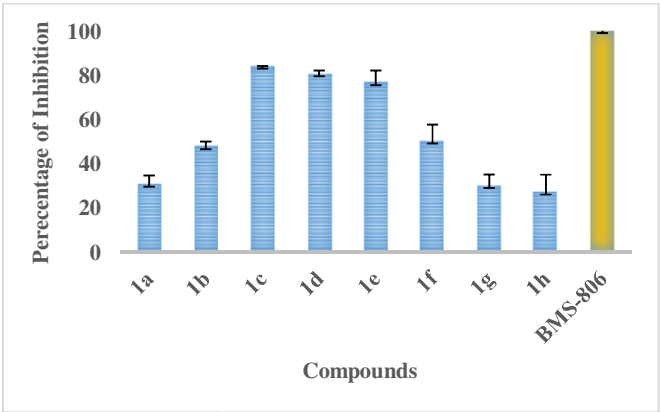

Scheme 2. Inhibitory activity for 1,4-DHP derivatives at 100 µM

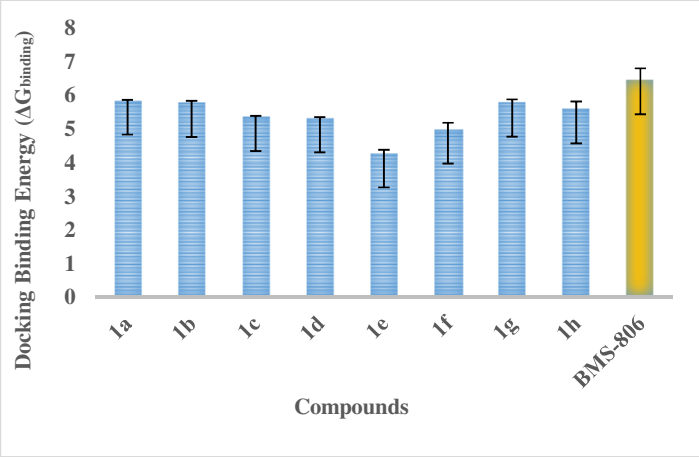

Scheme 3. Docking binding energy ($\Delta G_{binding}$) for 1,4-DHP derivatives in comparison with **BMS-806**

Conclusions

In the present study, 4-arylpyridin-1(4*H*)-yl) benzoic acid was introduced as a novel anti-HIV-1 scaffold. Eight different derivatives of 4-(3,5-bis(alkoxycarbonyl)-2,6-dimethyl-4-arylpyridin-1(4*H*)-yl)benzoic acid were designed and synthesized as anti-HIV-1 agents. After structural elucidation by FT-IR, ^{1}H-NMR, LC-Mass and elemental analysis, the anti-HIV-1 activity of all compounds was evaluated. Most of the studied compounds were moderate to good anti-HIV-1 agents lacking considerable cytotoxicity in cell cultures. The most potent compounds (**1c**, **1d** and **1e**) exhibited 84, 80.5 and 76.42% HIV-1 inhibitory activity at 100 µM, respectively. Structure-activity relationships analysis revealed that the presence of 2-furyl and 2- thienyl hetero-aromatic substituents at the C4 position of 1,4-DHP ring enhanced the anti-HIV-1 activity and lowered the cytotoxic effect on MT-2 cell line. All of the compounds (**1a-h**) obeyed the Lipinski's "rule of five" and showed drug-likeness in terms of their ADMET profile.

Molecular docking simulation of the interaction with gp41 was carried out to investigate the posible inhibition of this protein with the prepared compounds. Docking simulation studies have revealed that 4-(3,5-bis(alkoxycarbonyl)-2,6-dimethyl-4-arylpyridin-1(4*H*)-yl)benzoic acids are bound mainly within gp41 binding site and the change in free energy of binding ($\Delta G_{binding}$) for most of the compounds was similar to that of NB-2. Autodock 4.2 estimated $\Delta G_{bindings}$ were correlated with the experimental in vitro anti-HIV-1 activities. Docking study indicated that all of the derivatives form electrostatic interactions and at least one H-bond with the gp41 binding site residues. These interactions were presumably associated with improved binding energies. Based on the obtained results, 1,4-dihydropyridine scaffold seems to be a promising candidate for the development of new HIV-1 inhibitors and **1c** and **1e** might be appropriate compounds for further modification towards more potent and selective anti HIV-1 agents.

Experimental Section

Chemistry

All chemicals, reagent and solvents were obtained from commercial suppliers and were freshly used after purification by standard procedures. Melting points were determined on the Electrothermal 9200 Melting Point apparatus and were uncorrected. ^{1}H-NMR spectra were recorded in DMSO-d_6 on a Bruker-Ultrashield 400MHz spectrometer (Germany). All the chemical shifts were reported as (δ) values (ppm) against tetramethylsilane as an internal standard. Electrospray mass spectra (ESI-Mass) were obtained in negative and positive ion mode on a SHIMADZU LCMS-2010 EV spectrometer using methanol as solvent, a capillary voltage of 4500 V and a cone voltage of 10 V. FT-IR (KBr) spectra were recorded on a JASCO 6300 (Japan). Elemental analysis was performed using CHNS-923 LECO analyzer (USA) and the results were within ±0.4% of the theoretical values. All the experiments were monitored by analytical thin layer chromatography (TLC) on pre-coated silica gel 60 F254 aluminum plates (Merck, Germany). Preparative column chromatographies were carried out on silica gel (230–400 mesh, G60 F254 Merck, Art. 5715). Preparative thin-layer chromatography was done with prepared glass-backed plates (20×20 cm^2, 500 µm) using silica gel (Merck Kieselgel 60 HF254, Art. 7739). Suitable names for all the novel compounds were given with the aid of ChemOffice 2010 software. All final products were prepared in 25-58% yield. Their purity was determined by thin layer chromatography using several solvent systems of different polarities and ^{1}H-NMR and CHNOS analysis results.

They were all stable in refrigerator under 5 ˚C and in the darkness. General structure and structural details of the prepared compounds are summarized in Table **6**.

Table 6. General structure and structural features of the designed compounds

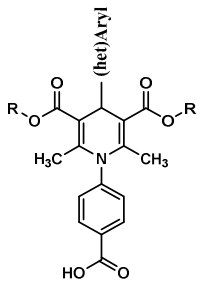

(1a-h)

Compound	(het)Aryl	R	Mol. formula	Mol. weight
1a	Styryl	CH_3	$C_{26}H_{25}NO_6$	447.48
1b	4-Dimethylaminophenyl	CH_3	$C_{26}H_{28}N_2O_6$	464.51
1c	2-Furyl	CH_3	$C_{22}H_{21}NO_7$	411.40
1d	2-Furyl	C_2H_5	$C_{24}H_{25}NO_7$	439.46
1e	2-Thienyl	CH_3	$C_{22}H_{21}NO_6S$	427.47
1f	2-Thienyl	C_2H_5	$C_{24}H_{25}NO_6S$	455.52
1g	5-Nitro-2-furyl	CH_3	$C_{22}H_{20}N_2O_9$	456.40
1h	Phenyl	CH_3	$C_{24}H_{23}NO_6$	421.44

*General procedure for the synthesis of 4-(3,5-bis(alkoxycarbonyl)-2,6-dimethyl-4-arylpyridin-1(4H)-yl)benzoic acid (**1a-h**)*

A mixture of corresponding aldehyde (3.0 mmol), alkyl acetoacetate (6.0 mmol) and *para*-aminobenzoic acid (3.0 mmol) in ethanol (4 mL) was heated and stirred under reflux. The progress of the reaction was monitored by TLC. After completion of the reaction, the reaction mixture was cooled to room temperature then ethanol was removed under reduced pressure and the product was left overnight in freezer. The obtained solid was filtered off, washed with small portions of cold ethanol and crystallized from ethanol to give compounds **1a-h**. For compounds **1c** and **1d**, the process of purification was different: after cooling the mixture, ethanol was removed under reduced pressure and the product was purified by column chromatography over silica gel using chloroform-methanol. In the case of compounds **1b** and **1h**, one milliliter of HCl was used as catalyst in the reaction progress. After the completion of the reaction, the reaction mixture was cooled to room temperature, 5 mL of water was added, and the resulting mixture was extracted with chloroform (3×10 mL). The organic layers were combined and dried over anhydrous $MgSO_4$. After filtering the solid off, the solvent was removed under reduced pressure and the residue was purified by preparative TLC using chloroform-methanol as eluent. All the obtained products were completely dried in a vacuum oven.

The spectral features of the prepared molecules are provided in detail as follows.

*(E)-4-(3,5-Bis(methoxycarbonyl)-2,6-dimethyl-4-styrylpyridin-1(4H)-yl)benzoic acid (**1a**)*

Yellow crystals. Yield: 25%.M.p.194-195 ˚C. FT-IR (KBr) ν (cm^{-1}): 2500-3500 (O-H, acid), 2956.34 (C-H, aromatic), 2832.92 (C-H, aliphatic), 1686.44 (C=O, ester), 1654.32 (C=O, acid), 1626.66 (C=C, alkene), 1600.63 & 1571.70 (C=C, aromatic), 1273.75 (C-O, ester), 1166.72 (C-O, acid). ^{1}H-NMR (DMSO-d_6) δ (ppm): 10.63 (1H, s: COOH), 7.95 (2H, d, *J*=8.4 Hz, C3-H, C5-H: -C_6H_4COOH), 7.67 (2H, d, *J*=8.4 Hz, C2-H, C6-H: -C_6H_4COOH), 7.31-7.34 (5H, m, C2-H, C3-H, C4-H, C5-H, C6-H: -CH=CHC_6H_5), 6.59-6.61 (2H, m, Ca-H, Cb-H: -HCa=CbHC_6H_5), 4.89 (1H, s, C4-

H: DHP), 3.67 (6H, s: 2×-$COOCH_3$), 2.21 (6H, s, C2-CH_3, C6-CH_3: DHP). Mass m/z (%): 446.30 (M-1). Anal. Calcd. for $C_{26}H_{25}NO_6$ (447.48): C, 69.79; H, 5.63; N, 3.13; found: C, 69.67; H, 5.67; N, 3.21.

*4-(4-(4-(Dimethylamino)phenyl)-3,5-bis(methoxycarbonyl)-2,6-dimethylpyridin-1(4H)-yl)benzoic acid (**1b**)*

Yellow precipitates, Yield 58%.m.p.: 259-260 °C. FT-IR (KBr) ν (cm^{-1}): 2500-3200 (O-H, acid), 2882.70 & 2829.06 (C-H, aliphatic), 1686.44 (C=O, ester), 1658.55 (C=O, acid), 1627.63 & 1599.66 & 1422.24 (C=C, aromatic), 1272.79 (C-O, ester), 1165.76 (C-O, acid). ^{1}H-NMR (DMSO-d_6) δ (ppm): 12.76 (1H, brs: COOH), 7.94 (2H, d, *J*=8.4 Hz, C3-H, C5-H: -C_6H_4COOH), 7.76 (2H, d, *J*=9.2 Hz, C2-H, C6-H: -C_6H_4COOH), 7.24 (2H, d, *J*=8.4 Hz, C2-H, C6-H: -$C_6H_4N(CH_3)_2$), 6.79 (2H, d, *J*=8.8 Hz, C3-H, C5-H: -$C_6H_4N(CH_3)_2$), 5.31 (1H, s, C4-H: DHP), 3.68 (6H, s: 2×-$COOCH_3$), 3.02 (6H, s: -$C_6H_4N(CH_3)_2$), 2.03 (6H, s, C2-CH_3, C6-CH_3: DHP). Mass m/z (%): 463.15 (M-1). Anal. Calcd. (%) for $C_{26}H_{28}N_2O_6$ (464.51): C, 67.23; H, 6.08; N, 6.03. Found: C, 67.38; H, 6.09; N, 6.07.

*4-(4-(Furan-2-yl)-3,5-bis(methoxycarbonyl)-2,6-dimethylpyridin-1(4H)-yl)benzoic acid (**1c**)*

Pale yellow precipitates, Yield 51% m.p.: 248-249 °C. FT-IR (KBr) ν (cm^{-1}): 2500-3200 (O-H, acid), 3067.23 (C-H, aromatic), 2925.48 & 2867.02 (C-H, aliphatic), 1704.76 (C=O, ester), 1677.77 (C=O, acid), 1601.59 &1521.56 (C=C, aromatic), 1291.11 (C-O, ester), 1171.64 (C-O, acid). ^{1}H-NMR (DMSO-d_6) δ (ppm): 11.97 (1H, s: COOH), 7.89 (2H, d, *J*=8.8 Hz, C3-H ,C5-H: -C_6H_4COOH), 7.77 (2H, d, *J*=8.8 Hz, C2-H, C6-H: -C_6H_4COOH), 7.38 (1H, d, *J*=8.8 Hz, C3-H: furan), 6.74 (1H, d, *J*=8.8 Hz, C4-H: furan), 6.59 (1H, d, *J*=8.8 Hz, C5-H: furan), 5.91 (1H, brs, C4-H: DHP), 3.71 (6H, s: 2×-$COOCH_3$), 2.06 (6H, s, C2-CH_3, C6-CH_3: DHP). Mass m/z (%): 410.15 (M-1). Anal. Calcd. (%) for $C_{22}H_{21}NO_7$ (411.40): C, 64.23; H, 5.14; N, 3.40. Found: C, 64.59; H, 4.81; N, 3.68.

*4-(3,5-Bis(ethoxycarbonyl)-4-(furan-2-yl)-2,6-dimethylpyridin-1(4H)-yl)benzoic acid (**1d**)*

Pale yellow precipitates, Yield 51%.m.p.: 248-249 °C. FT-IR (KBr) ν (cm^{-1}): 2500-3200 (O-H, acid), 3064.33 (C-H, aromatic), 2899.45 (C-H, aliphatic), 1739.49 (C=O, ester), 1709.59 (C=O, acid), 1672.95 & 1604.48 (C=C, aromatic), 1284.36 (C-O, ester), 1174.44 (C-O, acid). ^{1}H-NMR (DMSO-d_6) δ (ppm): 12.32 (1H, s: COOH), 7.84 (2H, d, *J*=8.8 Hz, C3-H ,C5-H: -C_6H_4COOH), 7.72 (2H, d, *J*=8.8 Hz, C2-H, C6-H: -C_6H_4COOH), 7.37 (1H, d, *J*=8.8 Hz, C3-H: furan), 6.96 (1H, d, *J*=2.8 Hz, C4-H: furan), 6.82 (1H, d, *J*=7.6 Hz, C5-H: furan), 5.89 (1H, brs, C4-H: DHP), 4.80 (4H, q, *J*=4.4 Hz: $COOCH_2CH_3$), 2.89-2.90 (6H, m: $COOCH_2CH_3$), 2.10 (6H, s, C2-CH_3, C6-CH_3: DHP). Mass m/z (%): 438.20 (M-1). Anal. Calcd. (%) for $C_{24}H_{25}NO_7$ (439.46): C, 65.59; H, 5.73; N, 3.19. Found: C, 65.38; H, 5.45; N, 2.91.

*4-(3,5-Bis(methoxycarbonyl)-2,6-dimethyl-4-(thiophen-2-yl)pyridin-1(4H)-yl)benzoic acid (**1e**)*

White precipitates, Yield 46%.m.p.: 246-247 °C. FT-IR (KBr) ν (cm^{-1}): 2500-3200 (O-H, acid), 2999.73 (C-H, aromatic), 2949.59 & 2843.52 (C-H, aliphatic), 1698.98 (C=O, ester), 1639.20 (C=O, acid), 1598.70 & 1585.20 & 1429.96 (C=C, aromatic), 1275.68 (C-O, ester), 1205.29 (C-O, acid). ^{1}H-NMR (DMSO-d_6) δ (ppm): 13.27 (1H, s: COOH), 8.07 (2H, d, *J*=8.4 Hz, C3-H ,C5-H: -C_6H_4COOH), 7.41 (2H, d, *J*=8.4 Hz, C2-H, C6-H: -C_6H_4COOH), 7.30 (1H, d, *J*=5.2 Hz, C3-H: thiophen), 6.94 (1H, dd, *J*=4.0 Hz & *J*=2.0 Hz, C4-H: thiophen), 6.85 (1H, d, *J*=3.2 Hz, C5-H: thiophen), 5.31 (1H, s, C4-H: DHP), 3.67 (6H, s: 2×-$COOCH_3$), 2.00 (6H, s, C2-CH_3, C6-CH_3: DHP). Mass m/z (%): 426.15 (M-1). Anal. Calcd. (%) for $C_{22}H_{21}NO_6S$ (427.47): C, 61.81; H, 4.95; N, 3.28; S, 7.50. Found: C, 62.15; H, 5.12; N, 3.29; S, 7.82.

*4-(3,5-Bis(ethoxycarbonyl)-2,6-dimethyl-4-(thiophen-2-yl)pyridin-1(4H)-yl)benzoic acid (**1f**)*

White precipitates, Yield 41%. m.p.: 242-243 °C. FT-IR (KBr) ν (cm^{-1}): 2500-3200 (O-H, acid), 2956.34 (C-H, aromatic), 2832.92 (C-H, aliphatic), 1704.76 (C=O, ester), 1676.80 (C=O, acid), 1600.63 & 1524.45 & 1421.28 (C=C, aromatic), 1293.04 (C-O, ester), 1175.40 (C-O, acid). ^{1}H-NMR (DMSO-d_6) δ (ppm): 12.93 (1H, brs: COOH), 8.04 (2H, d, *J*=8.4 Hz, C3-H ,C5-H: -C_6H_4COOH), 7.39 (2H, d, *J*=8.4 Hz, C2-H, C6-H: -C_6H_4COOH), 7.29 (1H, dd, *J*=1.2 Hz, *J*=4.0 Hz, C3-H: thiophen), 6.93 (1H, dd, *J*=4.0 Hz & *J*=2.0 Hz , C4-H: thiophen), 6.83 (1H, d, *J*=3.2 Hz, C5-H: thiophen), 5.08 (1H, s, C4-H: DHP), 3.99 (4H, q, *J*=2.8 Hz: $COOCH_2CH_3$), 2.50-2.51 (6H, m: $COOCH_2CH_3$), 2.03 (6H, s, C2-CH_3, C6-CH_3: DHP). Mass m/z (%): 454.15 (M-1). Anal. Calcd. (%) for $C_{24}H_{25}NO_6S$ (455.52): C, 63.28; H, 5.53; N, 3.07; S, 7.04. Found: C, 62.93; H, 5.25; N, 3.38; S, 7.41.

*4-(3,5-Bis(methoxycarbonyl)-2,6-dimethyl-4-(5-nitrofuran-2-yl)pyridin-1(4H)-yl)benzoic acid (**1g**)*

Pale yellow precipitates, Yield 35%.m.p.: 191-192 °C. FT-IR (KBr) ν (cm^{-1}): 2800-3400 (O-H, acid), 3000.69 (C-H, aromatic), 2955.38 & 2832.92 (C-H, aliphatic), 1687.41 (C=O, ester), 1658.55 (C=O, acid), 1628.66 & 1599.66 & 1420.32 (C=C, aromatic), 1385.60 (N-O, Nitro), 1271.82 (C-O, ester), 1164.79 (C-O, acid). ^{1}H-NMR (DMSO-d_6) δ (ppm): 12.79 (1H, s: COOH), 10.58 (1H, brs, C4-H: furan), 8.86 (1H, brs, C5-H: furan), 7.89 (2H, d, *J*=8.4 Hz, C3-H ,C5-H: -C_6H_4COOH), 7.27 (2H, d, *J*=8.8 Hz, C2-H, C6-H: -C_6H_4COOH), 4.83 (1H, s, C4-H: DHP), 3.61 (6H, s: 2×-$COOCH_3$), 2.15 (6H, s, C2-CH_3, C6-CH_3: DHP). Mass m/z (%): 455.15 (M-1). Anal. Calcd. (%) for $C_{22}H_{20}N_2O_9$ (456.40): C, 57.90; H, 4.42; N, 6.14. Found: C, 58.21; H, 4.72; N, 6.23.

*4-(3,5-Bis(methoxycarbonyl)-2,6-dimethyl-4-phenylpyridin-1(4H)-yl)benzoic acid (**1h**)*

White crystals, Yield 31%. m.p.: 213-215 °C. FT-IR (KBr) ν (cm^{-1}): 2500-3200 (O-H, acid), 3046.98 (C-H, aromatic), 2905.24 (C-H, aliphatic), 1705.73 (C=O, ester), 1609.31 (C=O, acid), 1576.52 & 1505.17 (C=C, aromatic), 1246.75 (C-O, ester), 1114.65 (C-O, acid). ^{1}H-NMR (DMSO-d_6) δ (ppm): 11.97 (1H, brs, COOH), 7.63 (2H, d, *J*=2.0 Hz, C3-H ,C5-H: -C_6H_4COOH), 7.23-7.27 (3H, m, C3-H, C4-H, C5-H: phenyl), 7.17 (2H, d, *J*=6.4 Hz,C2-H, C6-H: phenyl), 6.54 (2H, d, *J*=8.4 Hz, C2-H, C6-H: -C_6H_4COOH), 5.88 (1H, s, C4-H: DHP), 3.68 (6H, s, 2×$COOCH_3$), 2.17 (6H, s, C2-CH_3, C6-CH_3: DHP). Mass m/z (%): 420.15 (M-1). Anal. Calcd. (%) for $C_{24}H_{23}NO_6$ (421.44): C, 68.40; H, 5.50; N, 3.32. Found: C, 68.69; H, 5.41; N, 3.39.

Biological assay

Inhibition of the HIV-1 entry by the prepared compounds was investigated. **BMS-806** as the control HIV-1 surface glycoprotein inhibitor was used in the experiments.[25] Synthesized compounds were dissolved in dimethyl sulfoxide (DMSO) at different concentrations. DMSO with the final concentration of 1% V/V (1 mL DMSO in 100 mL H_2O) was considered as the negative solvent control. DMSO plus MT-2 (human lymphocyte) cells and virus were used to normalize the solvent effect.[26] **BMS-806** (200 mM) was dissolved in DMSO and kept in -20°C. All tests were performed in triplicate.

Inhibition of HIV-1 single-cycle infection

Human embryonic kidney (HEK) and MT-2 cells were obtained from National Cell Bank of Iran. MT-2 cells were produced by co-culturing normal human cord leukocytes with leukemic T-cells from a patient with adult T-cell leukemia. To measure the inhibition effect, HEK 293T cells were cultured in RPMI 1640 and DMEM (Dulbecco's modified Eagle's medium) containing 15% L-FBS (Fetal Bovine Serum), 100 U/mL of penicillin, and 100 µg/mL of streptomycin.[27] In the step of transfection into HEK cells, HEPES (4-(2-hydroxyethyl)-1-piperazine ethane sulfonic acid) was added and finally the cells were incubated at 37 °C under 5% CO_2.

To produce the SCR HIV-1 virions, pMD2G, pmzNL4-3 and pSPAX2 plasmids were used. These plasmids were co-transfected into HEK 293T cells in 6-well plates (5×105 cells/well) in certain proportion using PolyFect reagent (Qiagen) according to the suggested method by Qiagen. Supernatants of the transfected cells were harvested after 24, 48 and 72 h after infection and fresh medium was added to the culture wells. Mediums containing viruses were mixed together and stored at -70 °C after filtration with 0.22 µm filters.[28] Final centrifugation on the filtrate at 60,000 g was performed for 2 h at 4 °C. The supernatant was taken out and the virions pellet was shaken gently overnight in 1/30 volume of RPMI 1640 at 4 °C. SCR HIV-1 virions were produced in 24-well plates to generate viruses for measuring the rate of production and maturation. 70×103 HEK 293T cells were used for producing SCR HIV-1 virions by 400 ng of plasmid. Transfection was carried out in the presence of 4 µL of PolyFect reagent. Volume of transfection was 300 µL and the volume of the added DNA complex was 120 µL. When transfection was complete, 800 µL of the complete medium containing the synthesized compounds was added to the cells. The culture medium containing the virus was collected 48 h after transfection and the amount of the purified virus was measured using p24 ELISA assay kit (Cell Biolabs).[29]

Cytotoxicity assay

The toxicity of compounds for target cell (Hela) was assayed using XTT (sodium 3-[1 (phenylaminocarbonyl)-3,4-tetrazolium]-bis(4-methoxy-6-nitro)benzene sulfonic acid) (Roche, Germany) as described previously. The replication assay plates were directly subjected to XTT assay after analysis of supernatant for P24 load. Before addition of XTT, the medium was aspirated and replaced with phosphate-buffered saline (PBS). The XTT solution was prepared and added to the wells according to the user manual. Cell was then incubated for an additional 2 h to allow the formazan production. The optical densities were measured with ELISA reader at test and reference wave lengths of 492 nm and 690 nm, respectively.

In Silico studies

In silico calculation of physicochemical parameters and ADMET prediction

Lipinski's rule of five which is essential to ensure a drug-like pharmacokinetics profile and the physicochemical properties of the designed derivatives were assessed using online Osiris property explorer[30] and Molinspiration WebME Editor1.16.[31] These physicochemical properties were: calculated logarithm of partition coefficient (CLogP), logarithm of solubility (LogS), molecular weight (MW), drug-likeness, number of hydrogen bond donors (HBD), number of hydrogen bond acceptors (HBA), number of rotatable bonds (nROTB), drug score, topological polar surface area (TPSA). Absorption, distribution, metabolism and excretion (ADME) of the designed molecules were some more physicochemical properties calculated *in silico*.

Molecular docking studies

Molecular docking studies were carried out by AutoDock version 4.2.[32] The three-dimensional (3D) protein structure of gp41 (PDB ID: 1AIK), determined by X-ray crystallography, was retrieved from the RCSB Protein Databank.[33] The protein was then corrected by removing the extra crystallized water molecules using Accelrys discovery studio visualizer 4.0[34] and adding polar hydrogens and charges to the molecule byAutoDockTools version 1.5.6rc3.[21] Protonation step corrects the ionization and tautomeric states of residues and thus modifies the total Kollman charges on the protein structure. All two-dimensional (2D) structures of the ligands were drawn by ChemDraw program.[35] Each structure was energy minimized by MM^+ force field and PM3 semi-empirical techniques in HyperChem8 software. Then, partial charges of atoms were calculated using Gasteiger-Marsili procedure. Non-polar hydrogens of compounds were merged, rotatable bonds were assigned and finally the molecules were saved as pdbqt format file. The resulting protein structure was used as an input for the AutoGrid program. AutoGrid performs pre-calculated atomic affinity grid maps for each atom type in the ligand, plus an electrostatics map and a separate desolvation map presented in the substrate molecule. All maps were calculated with 0.375 Å spacing between grid points. Grid center was centered on the Cα atom of Lys574 residue with x=24.00, y=21.82 and z=23.82 coordinates obtained using Acceryls discovery studio visualizer 4.0. The location and size of the grid were set in a way to contain not only the active site but also considerable portions of the surrounding surface. For this purpose, box was set at 60×60×60 Å. Each docking was performed by 150 runs of the AutoDock search by the Lamarckian genetic algorithm (LGA). The factors for LGA were defined as follows: a maximum number of 5,000,000 energy evaluations; a maximum number of generations of 27,000; mutation and crossover rates of 0.02 and 0.8, respectively. Lastly, the conformation of the lowest predicted binding free energy of the most occurring binding modes in the gp41 binding site was selected. Graphic manipulations and visualizations were done by Accelrys discovery studio visualizer 4.0 software.

Statistical methods

Analysis of variance (ANOVA) was used as a technique for analyzing experimental data in which one or more response variables are measured under numerous conditions. In an analysis of variance, the difference in the response is divided into variation attributable to differences between the response variables and variation attributable to random error. A usual aim in ANOVA is to compare means of the response variable for various combinations of the classification variables. ANOVA table consists of sum-of-squares, degrees of freedom, mean square, F ratio and p values less than 0.05 which are considered statistically significant. ANOVA was done on the data to determine the significant variables of the docking and biological assay procedures.

References

[1]T. Tiefenbrunn, C. D. Stout, 'Towards novel therapeutics for HIV through fragment-based screening and drug design',*Prog. Biophys.Mol. Biol.***2014**, *116*, 124-140.

[2]P. Zhan, C. Pannecouque, E. D. Clercq, X. Liu, Anti-HIV Drug Discovery and Development: Current Innovations and Future Trends, *J. Med. Chem.***2016**, 59, 2849-2957.

[3] D. D. Richman, S. C. Morton, T. Wrin, N. Hellmann, S. Berry, M. F. Shapiro, S. A. Bozzette,The prevalence of antiretroviral drug resistance in the United States, *AIDS.***2004**, *18*, 1393-1401.

[4] C. F. Pereira, J. T. Paridaen, Anti-HIV drug development-An overview,*Curr. Pharm. Des.***2004**, *10*, 4005-4037.

[5] D. Yu, C. T. Wild, D. E. Martin, S. L. Morris-Natschke, C. H. Chen, G. P. Allaway, K. H. Lee, The discovery of a class of novel HIV-1 maturation inhibitors and their potential in the therapy of HIV, *Expert. Opin. Investig. Drugs.***2005**, *14*, 681-693.

[6] R. Blumenthal, S. Durell, M. Viard, HIV entry and envelope glycoprotein-mediated fusion, *J. Biol. Chem.***2012**, *287*, 40841-40849.

[7] M. L. Bosch, P. L. Earl, K. K. Fargnoli, S. Picciafuoco, F. Giombini, F. Wong-Staal, G. Franchini, Identification of the fusion peptide of primate immunodeficiency viruses, *Science*.**1989**, *244*, 694-697.

[8] J. D. Feo Christopher, W. Wang, M. L. Hsieh, M. Zhuang, R. Vassell, C. D. Weiss, Resistance to N-peptide fusion inhibitors correlates with thermodynamic stability of the gp41 six-helix bundle but not HIV entry kinetics, *Retrovirolog.***2014**, *11*, 86-97.

[9] S. Liu, S. Wu, S. Jiang, HIV entry inhibitors targeting gp41: from polypeptides to small-molecule compounds,*Curr. Pharm. Des.***2007**, *13*, 143-162.

[10] C. Teixeira, F. Barbault, J. Rebehmed, K. Liu, L. Xie, H. Lu, S. Jiang, B. T. Fan, F. Maurel, Molecular modeling studies of N-substituted pyrrole derivatives-potential HIV-1 gp41 inhibitors. *Bioorg. Med. Chem.***2008**, *16*, 3039-3048.

[11] S. Sepehri, S. Gharagani, L. Saghaie, M. R. Aghasadeghi, A. Fassihi, QSAR and docking studies of some 1,2,3,4-tetrahydropyrimidines: evaluation of gp41 as possible target for anti-HIV-1 activity, *Med. Chem. Res.***2015**, *24*, 1707-1724.

[12] G. Zhou, D. Wu, B. Snyder, R. G. Ptak, H. Kaur, M. Gochin, Development of indole compounds as small molecule fusion inhibitors targeting HIV-1 glycoprotein-41,*J. Med. Chem.***2011**, *54*, 7220-7231.

[13] A. R. Katritzky, S. R. Tala, H. Lu, A. V. Vakulenko, Q. Y. Chen, J. Sivapackiam, K. Pandya, S. Jiang, A. K. Debnath, Design, synthesis, and structure-activity relationship of a novel series of 2-aryl 5-(4-oxo-3-phenethyl-2-thioxothiazolidinylidenemethyl)furans as HIV-1 entry inhibitors, *J. Med. Chem.***2009**, *52*, 7631-7639.

[14] G. Zhou, D. Wu, E. Hermel, E. Balogh, M. Gochin, Design, synthesis, and evaluation of indole compounds as novel inhibitors targeting gp41, *Bioorg. Med. Chem. Lett.***2010**, *20*, 1500-1503.

[15] C. Pan, S. Liu, S. Jiang, J. Formos, HIV-1 gp41 fusion intermediate: a target for HIV therapeutics,*Med. Assoc.***2010**, *109*, 94-105.

[16] A. Hilgeroth, A. Billich,Cage Dimeric 4-Aryl-1,4-dihydropyridines as Promising Lead Structures for the Development of a Novel Class of HIV-1 Protease Inhibitors, *Arch. Pharm. Pharm. Med. Chem.***1999**, *332*, 3-5.

[17] A. Hilgeroth, M. Wiese, A. Billich, Synthesis and Biological Evaluation of the First N-Alkyl Cage Dimeric 4-Aryl-1,4-dihydropyridines as Novel Nonpeptidic HIV-1 Protease Inhibitors,*J. Med. Chem.***1999**, *42*, 4729-4732.

[18] A. Hilgeroth, H. Lilie, Structure-activity relationships of first bishydroxymethyl-substituted cage dimeric 4-aryl-1,4-dihydropyridines as HIV-1 protease inhibitors, *Eur. J. Med. Chem.***2003**, *38*, 495-499.

[19] A. Fassihi, Z. Azadpour, N. Delbari, L. Saghaie, H. R. Memarian, R. Sabet, A. Alborzi, R. Miri, B. Pourabbas, J. Mardaneh, P. Mousavi, B. Moinifard, H. Sadeghi-aliabadi, Synthesis and antitubercular activity of novel 4-substituted imidazolyl-2,6-dimethyl-N3, N5-biasryl-1,4-dihydropyridine-3,5-dicarboxamides,*Eur. J. Med. Chem.***2009**, *44*, 3253-3258.

[20] G. M. Morris, R. Huey, W. Lindstrom, M. F. Sanner, R. K. Belew, D. S. Goodsell, A. J. J. Olson, AutoDock4 and AutoDockTools4: Automated docking with selective receptor flexibility, *Comput. Chem.***2009**, *30*, 2785-2791.

[21] W. M. Kazmierski, T. P. Kenakin, K. S. Gudmundsson, Peptide, peptidomimetic and small-molecule Drug Discovery Targeting HIV-1 Host-cell Attachment and Entry through gp120, gp41, CCR5 and CXCR4, *Chem. Biol. Drug. Des.***2006**, *67*, 13-26.

[22] Y. Pan, R. A. Birdsey, J. Fang, R. Houghton, P. E. Kauppi, W. A. Kurz, O. L. Phillips, A. Shvidenko, S. L. Lewis, J. G. Canadell, P. Ciais, R. B. Jackson, S. W. Pacala, A. D. McGuire, S. Piao, A. Rautiainen, S. Sitch, D. Hayes, A Large and persistent carbon sink in the world's forests, *Science.***2011**, *333*, 988-993.

[23] Y. Wang, H. Lu, Q. Zhu, S. Jiang, Y. Liao, Structure-based design, synthesis and biological evaluation of new N-carboxyphenylpyrrole derivatives as HIV fusion inhibitors targeting gp41, *Bioorg. Med. Chem. Lett.***2010**, *20*, 189-192.

[24] S. Jiang, S. R. Tala, H. Lu, P. Zou, I. Avan, T. S. Ibrahim, N. E. Abo-Dya, A. Abdelmajeid, A. K. Debnath, A. R. Katritzky, *Bioorg. Med.Chem. Lett.***2011**, *21*, 6895.

[25] W. C. Olson, P. J. Maddon, Resistance to HIV-1 entry inhibitors, *Curr. Drug. Targets. Infect. Disord.***2003**, *3*, 283-294.

[26] M. Peeters, R. Vincent, J. L. Perret, M. Lasky, D. Patrel, F. Liegeois, V. Courgnaud, R. Seng, T. Matton, S. Molinier, E. Delaporte, Evidence for differences in MT-2 cell tropism according to genetic subtypes of HIV-1: syncytium-inducing variants seem rate among subtype C HIV-1 viruses, *J. Acquir. Immune. Defic. Syndr.***1999**, *20*, 115-120.

[27] A. Adachi, H. E. Gendelman, S. Koenig, T. Folks, R. Willey, A. Rabson, M. A. Martin, Production of acquired immunodeficiency syndrome-associated retrovirus in human and nonhuman cells transfected with an infectious molecular clone, *J. Virol.***1986**, *59*, 284-291.

[28] E. M. Campbell, O. Perez, M. Melar, T. J. Hope, Labeling HIV-1 virions with two fluorescent proteins allows identification of virions that have productively entered the target cell, *Virology.***2007**, *360*, 286-293.

[29] R. Zabihollahi, S. M. Sadat, R. Vahabpour, M. R. Aghasadeghi, A. Memarnejadian, T. Ghazanfari, M. Salehi, A. Rezaei, k. Azadmanesh, Development of single-cycle replicable human immunodeficiency virus 1 mutants, *Acta. Virol.***2011**, *55*, 15-22.

[30] http://www.organic-chemistry.org/prog/peo/

[31] http://www.molinspiration.com

[32] G. M. Morris, R. Huey, A. J. Olson, Using AutoDock for ligand-receptor docking. Current Protocols in Bioinformatics, *Curr. Protoc.Bioinformatics.***2008**, Chapter 8, Unit 8, 14.

[33] http://www.rcsb.org/pdb/home/home.do

[34] DSVisualizer, Accelrys Software Inc. San Diego CA USA 2014

[35] ChemDraw Ultra10.0, Cambridge soft.

Entry for the Table of Contents ((required for publication))

((Insert TOC Graphic here; max. width: 17.5 cm; max. height: 7.0 cm))